International Journal of Materials Chemistry and Physics
Vol. 1, No. 1, 2015, pp. 31-42
http://www.aiscience.org/journal/ijmcp

Hydrothermal Synthesis of Nanostructured Materials for Energy Harvesting Applications

Radu-Robert Piticescu[1, *], Adrian Mihail Motoc[1], Albert Ioan Tudor[1], Cristina Florentina Rusti[1], Roxana Mioara Piticescu[1], Maria Dolores Ramiro-Sanchez[2]

[1]National Institute for Nonferrous and Rare Metals, Pantelimon-Ilfov, Romania
[2]AIDICO-Technological Institute for Construction, Novelda, Alicante, Spain

Abstract

Hydrothermal synthesis is one a chemical method with high potential for obtaining nanostructured materials with controlled properties for energy harvesting applications. The main advantage of the hydrothermal processes is the ability to control nucleation and growth in complex systems containing a large number of components and dopants, without affecting the structural and morphological homogeneity. This is leading to some important technological and environmental advantages such as: one step process for direct production of crystalline ceramic powders, low energy consumption, products with much higher homogeneity than classical solid state processing, versatility in producing oxides, non-oxides and hybrid materials with different morphologies, possibility to be up-scaled to pilot and production levels. These features are proved for some selected nanomaterials with high impact in energy harvesting technologies: yttria doped zirconia nanomaterials for solid oxide fuel cells, lead zirconate titantate (PZT) used as piezoelectric materials in sensors, transducers and actuators, BST perowskite structures for sensors applications and zinc oxide as nanomatrix for encapsulating phase change materials in energy storage. The development of these complex materials was based on thermodynamic approaches and modelling methods to optimize the grain size and microstructure. Based on these approaches, future developments are expected to show the scalability of the processes from laboratory to pilot and industrial scale, thus opening new directions in the energy harvesting field.

Keywords

Nanostructures, Hydrothermal Synthesis, Thermodynamic Prediction, Modelling

Received: May 26, 2015 / Accepted: June 19, 2015 / Published online: July16, 2015

1. Thermodynamic and Kinetic Approaches in Hydrothermal Synthesis of Nanomaterials

Nanomaterials are one of the "key-enabling technologies" of today and tomorrow industry due to their huge and global impact in all production sectors such as information and communications technology, medicine and pharmacy, constructions and buildings, energy and transportation, aerospace and defense [1]. Nanostructured materials science and technology is a broad and multidisciplinary field of research linked to both emerging applications and modernization of traditional sectors in recent years, explaining the continuous growing research interest. Nanostructured materials are defined as materials having at least one dimension < 100 nm (usually less than 50 nm) and include atomic clusters (0D), filamentary structures (1D), layered (lamellar) films (2D), and bulk nanostructured materials (3D). The law dimensionality and related high surface to volume atoms ratio lead to physical or chemical properties that can be very different from the macroscale

* Corresponding author
E-mail address: rpiticescu@imnr.ro (R. R. Piticescu)

properties of the same substance [2]. The so called "triangle synthesis – properties – applications" must be fully exploited to obtain assessed materials for applications, due to the correlations with their atomic structure, composition, microstructure, defects and interfaces, which are controlled by thermodynamics and kinetics of the synthesis process.

Different synthesis routes for manufacturing of nanomaterials have been proposed. Generally they may be classified in physical, chemical and combined routes. Other classification considers the top-down approach from the macroscale to the nanoscale, or conversely, by assembly of atoms or particles using the bottom-up approach.

Chemical reactions for material synthesis can be done in solid (conventional synthesis route), liquid or gaseous state. For solid state reactions, diffusion of atoms depends on the temperature of the reaction and transport across grain boundaries and grain growth at elevated reaction temperature may lead to solids with large grain size. Compared to solid-state synthesis, diffusion in the liquid or gas phase is typically many orders of magnitude larger than in the solid phase; thus the synthesis of nanostructured materials can be achieved at lower temperatures, reducing the detrimental grain growth.

Water is one of the best known and the most common solvents used in the acid/base reaction, precipitation or reduction/oxidation (redox). In chemical synthesis of materials, one should always use caution when handling reactants and precursors, reaction by-products and post-reaction wastes, particularly when complex and hazardous chemicals are involved.

Although many laboratory-scale reactions can be scaled up to economically produce large quantities of materials, the laboratory-scale reaction parameters may not be linearly related to that of the large-scale reaction. The synthesis parameters such as temperature, pH, reactant concentration and time should be ideally correlated with factors such as super-saturation, nucleation and growth rates, surface energy and diffusion coefficients, in order to ensure the reproducibility of the process.

Hydrothermal treatment is one of the chemical synthesis methods with high potential for obtaining nanostructured materials with controlled properties. The hydrothermal chemistry is responsible for the formation of many minerals. The success of the researchers in the hydrothermal synthesis of big quartz piezoelectric mono-crystals have stimulated the development of fundamental studies in the physical-chemical synthesis of hydrothermal solutions. The hydrothermal processes used in the synthesis of nanostructured oxide precursors may be classified in [3]:

- Hydrothermal reactions, namely the synthesis of an oxide compound by the reactions of soluble precursors in solutions;
- Hydrothermal treatment for the purification or structural transformation of materials previously prepared by other methods;
- Hydrothermal growth of the crystals by controlling the dissolution – reprecipitation in solutions.

Hydrothermal synthesis reactions represent "in-situ" deprotonation of the water molecules from the first coordination sphere of the metallic cation due to the high temperatures and pressures in the hydrothermal solutions [4].

$$M_m[(H_2O)_n]^{Z+} \xrightarrow{T,p} [M_m(H_2O)_{mn-q}(OH)_q]^{(mz-q)+} + qH^+ \quad (1)$$

The hydrolysis reaction (1) describes a homogeneous nucleation process and the species formed represent the nucleation and growth sites leading to the formation of the new phase. From the thermodynamic point of view the equilibrium constant of the reaction (1) may be estimated from:

$$-RT \ln K_J = \sum_{i=1}^{nJ} \nu_i^{(J)} G_f^o\left(A_i^J\right) \quad (2)$$

Where: K_J = equilibrium constant of the reaction "J" in the system

A_i^J = species "i" participant in reaction "J"

ν_i^J = stoichiometric coefficient of species A_i^J

G_f^o =Gibbs chemical potential for the formation of species

n_J = total number of species in the system

R = ideal gases constant (8,314 J cal^{-1} K^{-1})

T = absolute temperature K

The exact calculation of the equilibrium constants in high pressure solutions requires specific thermodynamic approaches and the application of the Helgeson-Kircham-Flower (HKF) method. According to this apporach any thermodynamic property of solvated species M_pX_n or ions (M^{n+}, X^{p-}) is the sum of 2 terms: one for its intrinsic property (non-solvated) and the other one taking into account the contribution of the interactions solvate species (ion)/solvent (solvation) [5].

The kinetic of hydrothermal nucleation and growth may be studied based on Avrami-Erofeev equation:

$$x = 1 - \exp.\left(-kt^m\right) \quad (3)$$

$$k = \nu \exp.(-E_c / RT) \quad (4)$$

where x is the molar fraction from the new crystalline phase formed after the reaction time t, m is the reaction order, υ is the frequency factor and E_C the activation energy of crystallization. For m = 0.54 – 0.62 the reaction is in a diffusion controlled regime, for m = 1 the process is controlled by the formation of new interfaces and for m = 2 – 3 the nucleation and growth processes are the kinetic limiting steps. For hydrothermal reactions leading to phase transitions, the nucleation and growth processes are strongly influenced by the presence of anions (OH^-, SO_4^{2-}, NO_3^-, etc.), the existence of structural similarities between initial and final phase and existence of some critical sizes that stabilize the metastable phases. These general thermodynamic and kinetic analyses show the practical importance of studying the influence of the temperature, pressure, time, mineralizing agents and surface additives on the yield and final products properties [6].

The kinetic of solid species formation in hydrothermal solutions may be modelled considering the transfer of mineralizing reagent (ex. OH^- from alkaline mineralizers providing the required pH) from the solution to the surface of the nucleus (hydrous oxides initially formed) through the external adsorbed film, transfer of reagents through the new oxide layer formed at the interface and desorption of the reaction products into the solution volume. According to kinetic general rules of such topotactile processes and the corresponding un-reacted core model (fig. 1), the curve describing the degree of transformation vs. process duration may bring important information on the kinetic limiting step.

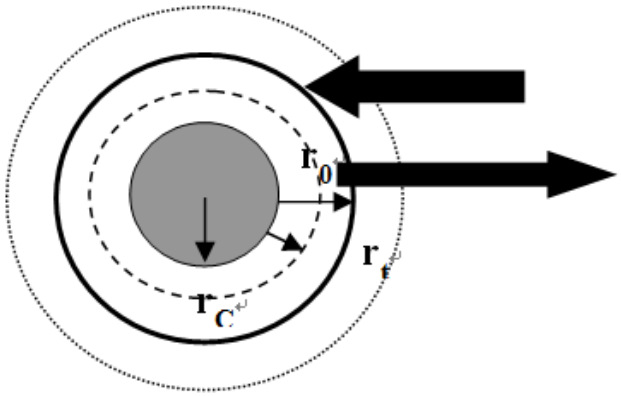

Fig. 1. The un-reacted core model for the kinetic study of transformation.

The symbols here are: r_C = the initial radius of the core particle; r_t = the radius of the particle at the time t from the process started; r_0 = the final radius of the particle.

According to this model, the steps of kinetic of the hydrothermal crystallization may be described by the following equations:

$$J_R = K_d^R 4\pi r_O C[X_R^V - X_R^i] \quad (5)$$

for the mass transfer of the reagent from the solution volume to the surface of the nuclei (hydrous oxides) through the external adsorbed solution film;

$$J_R = -\frac{4\pi r_O r_C}{(r_O - r_C)}(CD_R^{ef})[X_R^i - X_R^C] \quad (6)$$

For the mass transfer through the solid product layer, and

$$J_R = 4\pi r_i^2 C k_s [X_R^C - X_{RO}^{Ci} / K_e] \quad (7)$$

for the chemical transformation reaction at the interface.

The significance of the symbols in equations 5 to 7 are:

K_d^R – coefficient of mass transfer of reagent R trough the adsorbed solution film;

r_0 – initial radius of the particle

C – molar density of the reagent

X_R^v, X_R^i , X_R^C – molar fraction of reagent (volume, at interface and at un-reacted core)

X_{R0} – molar fraction of the new oxide formed

k_s – Kinetic constant of the chemical reaction

K_e – equilibrium constant of the reaction

2. Energy Harvesting Materials Developed by Hydrothermal Method

As a result of the main thermodynamic and kinetic features of the hydrothermal processes, the main advantages of the hydrothermal synthesis are:

- One step process for powder synthesis or oriented ceramic films;
- Minimized consumption of energy, particularly for complex and doped oxides;
- Products with much higher homogeneity than solid state processing;
- Products with higher density than gas or vacuum processing (faster growth rate);
- Versatility: oxides, non-oxides, organic/biologic materials, hybrid materials with different morphologies may be obtained;
- One of the few methods enabling obtaining of controlled doped or complex material systems.

The versatility of the hydrothermal method is demonstrated by the great number of compounds obtained via this processes. A non-exhaustive list comprises (starting from simple to complex oxides) contains: Al_2O_3, Fe_2O_3, SnO_2, TiO_2, ZrO_2, AlOOH, ErOOH, $K_4Nb_6O_{17}$, $K_2Ti_6O_{13}$, $KNbO_3$, $KTiNbO_3$, $KTaO_3$, Zn_2SiO_4, PbZr1-xTixO_3, Ba(Sr)Ti(Zr)O_3, $Ca_{0.8}Sr_{0.2}$Ti1-xFeO_3, (Fe, In)$_2O_3$(ITO), $LiFePO_4$, (Ce,Zr)O_2, YVO_4, (Co,Cu,Ni)(Fe,Co)$_2O_4$, YAG, $Mg_{3.5}H_2(PO_4)_3$, $CuAlO_2$, ZnO, $LiMn_2O_4$, LaxNiyO_3, (Ca,Mg)$(PO_4)_3$, etc, demonstrated by hydrothermal batch and flow reaction systems [7-22].

The hydrothermal technique is also well suited for non-oxides, such as pure elements (for example Si, Ge, Te, Ni, diamond, carbon nanotubes), selenides (CdSe, HgSe, $CoSe_2$, $NiSe_2$, $CsCuSe_4$), tellurides (CdTe, Bi_2Te_3, Cu_xTe_y, Ag_xTe_y), sulfides (CuS, ZnS, CdS, PbS, $PbSnS_3$), fluorides, nitrides (cubic or hexagonal BN), arsenides (InAs, GaAs), etc. [23].

A remarkable advantage of the hydrothermal synthesis is the significant effect on the solubility product of compounds in water at elevated temperatures and pressures. Also, the chemical reactivity of usually insoluble reagents can be strongly enhanced and the sluggish solid state reactions can be initiated in hydrothermal environment. Thirdly, the synthesis of 1 dimensional nanostructures can be done in facile conditions compared to other procedures [24].

A close look to the many materials developed via hydrothermal processes shows that many of these materials are of high importance in energy harvesting technologies and applications.

Doped $BaTiO_3$ (BT) and $PbZr_{1-x}Ti_xO_3$ (PZT) are key piezoelectric materials with applications in sensors, transducers and actuators, able to transform the mechanical vibrational energy in electricity. Other even more complex systems based on compounds like (Na,K)NbO_3 (KNN), Li(Nb,Ta,Sb)O_3 or their combinations such as KNN-$LiNbO_3$, KNN-$LiTiO_3$, KNN- Li(Nb,Ta,Sb)O_3, KNN-BT, KNN-$SrTiO_3$ have been developed as lead-free materials in the form of single crystals, polycrystalline ceramics and films to replace PZT, based on the unlimited possibilities to modify structure and properties by substitution and addition [25]. The application of piezoelectric vibration-based energy scavengers for converting mechanical energy to electrical energy are based on the utilization of piezoelectric generators and micro-power generators and are vital for the development of wireless sensors, low-power electronics, communication nodes and medical devices [26].

Magnetic nanomaterials are another class of materials used in energy harvesting technologies for many traditional or new emerging applications. Complex ferrites are already the core of electromagnetic devices while the development of nanostructures hybrid materials based on iron oxide and piezoelectric layered structures become indispensable solutions for energy harvesting in bio-micro-elecro-mechanics applications [27]. Semiconducting oxides like ZnO or TiO_2 doped with transitional metals (Co, Ni, Fe, Cr, etc.) having giant magneto resistance (GMR) are novel ferroelectric materials for spintronics [28].

Stabilized Y_2O_3–ZrO_2 ceramic (YSZ) is the most common solid electrolyte used in various applications as oxygen sensors and fuel cells. Their utilization made automotive industry more environment friendly due to its adequate level of oxygen ion conductivity and desirable stability in both oxidizing and reducing atmospheres. [29-31] NiO-YSZ composite powders were prepared by 2-step hydrothermal synthesis and applied as an anode functional layer to improve the performance of SOFCs [32].

Hydrothermal technology has also been recognized as an accessible technique for functionalization of carbon based materials, including functionalization of graphene for new types of sensors, batteries and other energy harvesting applications [33-35].

Some original results regarding the hydrothermal synthesis of doped zirconia nanomaterials for solid oxide fuel cells applications, barium strontium titanate perowskite structures and zinc oxide based nanomaterials for energy storage applications are presented below.

3. Hydrothermal Synthesis of Zirconia Nanomaterials

Zirconia (ZrO_2) is a ceramic material with very interesting and useful optical, electrical, thermal, hardness and biocompatibility properties. At temperatures below1100°C, monoclinic (*m*) phase of pure ZrO_2 is the stable form. From 1100°C up to 2370°C pure ZrO_2 has a tetragonal structure, but at temperatures between 2370°C and 2706°C (the melting point) it exists as cubic phase. The transition from tetragonal to monoclinic phase is done with a volume increase of about 4% leading to micro-cracking that drastically affects the mechanical properties. Therefore the stabilization of cubic or tetragonal phase on larger temperature ranges is required for safety application/reasons. The tetragonal or cubic phase can be stabilized (e.g. the temperature of the "$c \rightarrow t$" transition may be decreased), by introducing additives as MgO, CaO, Y_2O_3 and other rare earth oxides, etc. The doping elements do not affect only the structural and mechanical properties but also the optical and electrical behavior. Synthetically the binary system of ZrO_2 may be classified in [36, 37]: systems with formation of chemical compounds; systems forming cubic solid solutions in the rich ZrO_2 domain: ZrO_2 – MeO (Me = Mg, Cr, Co, Cu), ZrO_2 - Me_2O_3 (Me = Fe, Cr,La,),

ZrO_2 - Me_3O_4 (Me = Fe, Mn), ZrO_2 - MeO_2 (Me = Th, Ce); systems with the formation of other types of solid solutions in the rich ZrO_2 domain: HfO_2 - ZrO_2, TiO_2 - ZrO_2 and systems with no interactions between the components, e.g. ZnO - ZrO_2, Al_2O_3 - ZrO_2.

The ionic conductivity of doped zirconia materials in a large temperature range is the key property for energy harvesting applications in solid oxide fuel cells. To improve this property different approaches have been made: partial or total replacement of Y_2O_3 with Sc_2O_3 having a maximum corresponding to the composition $(Y_{0.5}Sc_{0.5})*0.3Zr_{0.7}O_{1.85}$, reducing the diffusion and transport distances using nanocrystalline membranes and thin films and development of composite ceramic materials with enhanced grain boundary conductivity [29-31].

The formation of ZrO_2 (as well as of the most of other oxides in hydrothermal solutions) takes place by a typical dissolution - reprecipitation process. For such types of transformations it is necessary to have a sufficient degree of super-saturation of the metallic cation in the solution acting as nucleation sites. Consequently, increasing the solubility of the Zr (IV) hydrated species one may expect to improve the kinetics of the new phase formation.

It was also reported that utilization of peroxo-precursors has important advantages in lowering ZrO2 synthesis temperature and improving kinetic conditions [38]. This was explained in terms of an increased solubility of the complex formed in the reaction:

$$\left[Zr_4(OH)_8\right]^{8+} + 12OH^- + 6H_2O_2 = 4\left[(HOO)Zr(OH)_6\right]^{2-} + 4H^+ \quad (8)$$

A simple method to estimate phase equilibrium during hydrothermal processes may be the analysis of potential-pH (Pourbaix diagrams). The graph below presented in figure 2 was done using the actual HSC v7 software. The calculation may be done at different initial metal concentrations while the pressure is automatically calculated on the basis of solution pressure at the given temperature. It shows that at the working temperature ZrO_2 solid species exists at pH>5. The software calculates the equilibrium diagram based on heat capacities, enthalpy and entropy of formation. Due to the lack of data regarding Y_2O_3-ZrO_2 solid solutions it is not possible to show its formation, however it is observed that at this temperature and pH range Zr and Y precipitate together as solid species and no soluble ions exist.

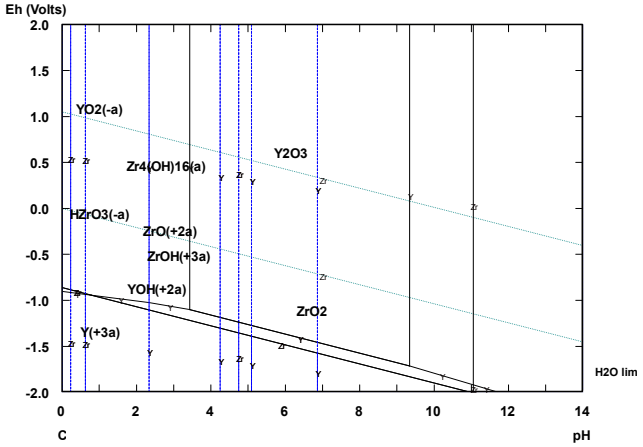

Fig. 2. Pourbaix diagram for the system Zr-Y-O-H at 250^{0}C, calculated with HSC v.7 software (Zr concentration 0.01M, Y_2O_3=3 mol %, autogenously pressure).

The hydrothermal synthesis of yttria-stabilized zirconia based on the mechanism proposed by the reaction (8) was done according to the procedure described in our paper [39]. The degree of crystallization of cubic ZrO_2 phase (X_c) and monoclinic phase (Xm) has been calculated from the ratios between the areas of the characteristic [111] peaks of samples and standard samples obtained by ammonia coprecipitation.

The mean crystallite sizes were calculated according to the Scherrer formula from the broadening of the [111] characteristic peak of the crystalline phases (table 1).

Table 1. Cubic zirconia crystallization from peroxide precursors [39].

Temperature (^{0}C)	Cubic		Monoclinic		Kinetic constants	
	Xc(%)	D_{111}(nm)	Xm(%)	D_{111}(nm)	K	N
125	21	7	-	-	$1.65x10^{-9}$	2.09
150	47	17	20	14	$3.47x10^{-8}$	1.871
175	69	19	26	22	$1.285x10^{-6}$	1.241
200	56	22	25	23	$2.698x10^{-5}$	1.308

In the temperature range 125–200^{0}C cubic zirconia phase has been formed, the degree of crystallization increasing with the time and temperature of the hydrothermal treatment (Table 1). Powders with large peaks, typically for the nanopowders have been prepared. Increasing temperature and time, the monoclinic zirconia phase has also been formed. The calculated mean crystallite sizes increased from about 6 nm to a maximum of 22 nm.

The kinetic constants of the crystallization process have been calculated using the equation proposed by Avrami in linear form:

$$\mathrm{n}\ln\frac{1}{1-X_c} = \ln k - n\ln t \tag{9}$$

where X_c is the fraction of the crystalline phase crystallized at the given time, k is the kinetic factor and n is the time exponent. The values obtained correspond to a diffusion-controlled crystallization process.

The formation of YTZP took place by hydrothermal crystallization of amorphous precipitated zirconia. The TEM presented in fig. 3 shows that powders preserve a structure similar to the chain structure of hydrous zirconia. This chain-like structure may explain the very high BET specific area between 195 to 200 m^2/g.

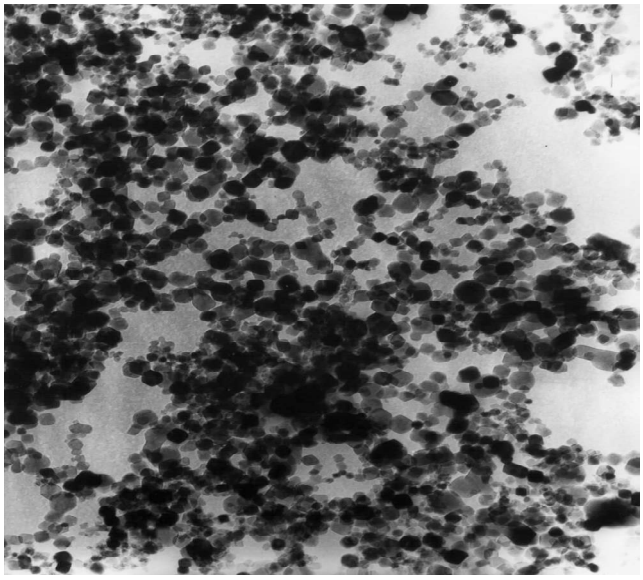

Fig. 3. TEM micrograph of hydrothermally synthesized 3 mol% Y_2O_3 - ZrO_2 powders [39].

Furthermore the same procedure has been developed to study the correlations between the hydrothermal synthesis parameters and the sintering behavior of YSZ nanopowders obtained by this procedure. Phase composition, calculated mean crystallite sizes (d_{111}) and particle sizes (D_p) for different hydrothermal treatment conditions showed that powders with large peaks, typical for the nanopowders have been prepared. The calculated mean crystallite sizes were in the range 8–23 nm, increasing with hydrothermal synthesis temperature and having a maximum in the neutral pH domain.

A mathematical correlation between the mean crystallite sizes, particle sizes and synthesis parameters (pH and temperature) could be derived by the minimum error analysis method using linear correlation analysis [40]. The mathematical model of the process was considered as a polynomial function $y_i = f_1(x_j)$, where y_i is the objective function or the problem restriction and x_j are the selected process parameters.

Linear dependence between the process realizations and parameters or second-order degree functions was considered:

$$y_i = \sum_{j=0} b_j x_j \ , \ y_1 = \sum_j b_j x_i + \sum_{j,k} b_{j,k} x_j x_k \tag{10}$$

Determination of the regression equations practically reduces to finding the maximum of a function of many variables by applying the less-square methods:

$$\frac{\partial \Phi_i}{\partial b_j} = 0 \ ,$$

where

$$\Phi_1 = \sum_{k=1}^{N} [\sum b_j x_{j,k} + \sum b_{j,k} x_{i,k} x_{j,k} - y_k] \tag{11}$$

Statistical analysis of the regression functions was done on the basis of Fischer criteria with the condition that calculated values to be less than the tabulated ones for the given number of parameters and restrictions.

Using this approach the following equations could be derived for the XRD mean crystallite size (Scherrer) and particle size (measured by dynamic laser scattering method)

$$d_{111} = -7.704 + 0.169\,pH + 0.109T \tag{12}$$

$$D_p = 0.6429 + 2.49\times10^{-2}\,pH - 1.5797\times10^{-3}\,T \tag{13}$$

As a conclusion, these studies show that YTZP powders with crystallite sizes in the range 8–22 nm have been obtained by hydrothermal treatment of amorphous hydrous oxides. The crystallization degree increases with hydrothermal treatment temperature, agglomeration degree decreasing with temperature increasing and pH decreasing. A mixture of tetragonal and cubic zirconia is formed, with increasing tetragonal phase content with decreasing pH.

YTZP powders obtained by the hydrothermal procedure having the microstructure and properties described before were used to obtain dense compact materials via two methods: bulk material by pseudo-axial pressing and sintering and tape casting of membranes followed by drying and sintering. The effective ionic conductivity of YTZP bulk materials was measured using impedance measurements**.** The contributions of bulk and grain boundaries on the total ionic conductivity were calculated from the impedance spectra of the samples. The results on the activation energy of ionic conduction are presented in table 2 and are in good agreement with the estimated values for YTZP nanomaterials.

Table 2. Activation energy of the ionic conductivity in YTZP nanomaterials.

Y_2O_3 mol% in YTZP	Grain sizes (nm)	Microstructure	Activation energy of ionic conductivity (kJ/mol)
7.5	625	Polycrystalline	110
3	524	Polycrystalline	97.5
3	393	Polycrystalline (0.25% Al_2O3 (grain growth inhibitor)	86
4	603	Polycrystalline	90
3		Single crystal	84

The results developed suggest that grain boundaries increase the total ionic conductivity of yttria-doped zirconia due to a "short circuit effect" leading to an apparent conductivity which is higher than of single crystals of similar composition [41]. This effect increases with decreasing grain sizes and may be practically neglected for large micrometric grain sizes.

4. Hydrothermal Synthesis of PZT and BST Perowskite Nanomaterials

Since the discovery of ferroelectric ceramics in the early 1940s (barium titanate capacitors), piezoelectrics market has reached several multibillion dollar on a market ranging from high-dielectric-constant capacitors to piezoelectric transducers, positive temperature coefficient devices or electro-optic devices. Materials based on two compositional systems, barium titanate and lead zirconate titanate, have dominated the field throughout their history. Various ceramic formulations, their form (bulk, films), method of fabrication and properties strongly influence their ferroelectric nature and specific areas of application [42].

The piezoelectric effect is related to an asymmetry in the unit cell and the resultant generation of electric dipoles due to the mechanical distortion. Lead zirconate titanate (PZT) is a solid solution phase of the $xPbZrO_3$ - (1-x)$PbTiO_3$ ($0<x<100$) binary system, with Ti and Zr atoms randomly occupying A-sites and Pb atoms situated at the corners of the unit cell with oxygen atoms located at the surface centers. For PZT ceramics the polarization is not spontaneous and a polling operation is required. After polling, the materials become ferroelectric up to the Curie temperature (T_C) when the crystalline lattice becomes symmetrical (cubic) and the piezoelectricity disappear. The direct piezoelectric effect is associated to the transformation of the electric charge to mechanical deformation and the reverse effect is transforming the mechanical deformation to electric charge. The piezoelectric properties are strongly influenced by doping with isovalent, donors or acceptor ions (table 3).

Table 3. Influence of dopants on the PZT ceramics properties.

Dopant type	Examples	Major effects
Isovalent	Ba^{2+}, Sr^{2+} replacing Pb^{2+} Sn^{4+} replacing Zr^{4+} or Ti^{4+}	Lower Curie temperature Higher permittivity
Donors (soft dopants)	La^{3+}, Nd^{3+}, Sb^{3+}, Bi^{3+} replacing Pb^{2+} Nb^{5+}, Ta^{5+}, Sb^{5+}, W^{6+} replacing Zr^{4+} or Ti^{4+}	Higher permittivity, higher coupling constant K_p, much lower mechanical quality factor Q_m, resistivity > 10^3
Acceptors (hard dopants)	K^+, Na^+ replacing Pb^{2+} Fe^{3+}, Al^{3+}, Sc^{3+}, In^{3+} Cr^{3+} replacing Zr^{4+} or Ti^{4+}	Lower permittivity, lower dielectric loss, lower coupling constant K_p, much higher mechanical quality factor Q_m

Soft dopants are required for actuators applications, therefore selection of doping elements should fall into this domain.

The microstructure of PZT ceramics depends on different factors such as grain sizes and grain boundaries, homogeneity, density and open porosity. Oxide dopants may control not only the ferroelectric properties but also inhibit (e.g. $Fe3^+$) or enhance (e.g. $Ce4^+$) the grain growth and therefore the density and the porosity. The selection of doping elements and their concentration may be predicted based on the tolerance factor defined by:

$$t = \frac{r_A + r_O}{\sqrt{2}(xr_B + r_O)} \quad (14)$$

where r_A is the covalent radius of Pb, Ti or Zr, r_B is the covalent radius of dopant B and x its molar concentration. A tolerance factor close to 1 is required to preserve the perowskite nature of the crystallite lattice. It is therefore expected that synthesis rout will affect the final properties of the sintered PZT ceramics.

The main problems for PZT powder synthesis routes are related to inhomogeneous distribution of dopants, grain sizes

and morphology. The one hydrothermal synthesis route based on thermodynamic design of the process eliminates or drastically reduces these problems.

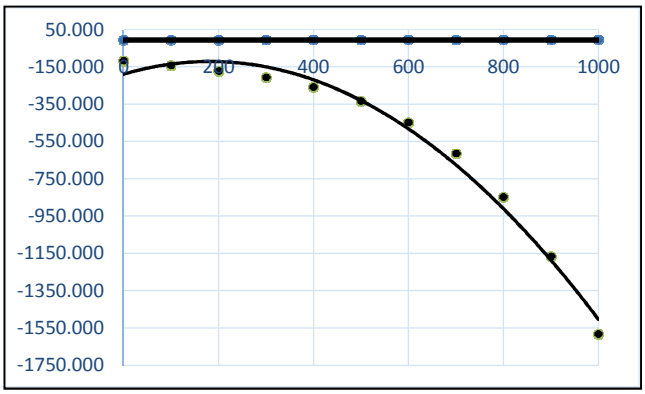

Fig. 4. The Gibbs free energy of formation of PZT from oxides (upper straight line) and from aqueous ions in hydrothermal solutions (lower polynomial line).

From the thermodynamic point of view, compared to classical ceramic route (solid phase mixing), the advantage of the process consists in a strong shift of the free energy toward much higher negative values presented in Fig. 4, as calculated with the HSC 7.1 thermodynamic software (Outokumpu, Finland).

The thermodynamic design of PZT materials shows the ability of hydrothermal process to obtain PZT powders with crystalline sizes < 43 nm by modeling crystallite growth according to equation (15):

$$Y_i = \ln(\ln\frac{1}{1-di/dm}) = -1.776 + 1.507\ln t_i \quad (15)$$

where d_i is the crystallite size in experimental point i and d_{max} is the maximum size after hydrothermal treatment at a certain pH and temperature.

Barium strontium titanate $Ba_{1-x}Sr_xTiO3$ (BST) is also a perowskite ceramic material with interesting applications in sensors and other devices [43]. The Curie temperature T_c of the BST compound can be controlled by varying the Ba/Sr ratio. At room temperature, when Ba amount is ranging between 0.7 – 1, the system is in ferroelectric phase, when Ba amount ranging between 0.1-0.7 the system is in paraelectric phase [44].

The properties of the BST based perovskites depend also on microstructure, grain size and defects [45]. The ferroelectric properties of the material decrease with grain size [46].

From the thermodynamic point of view, similar to PZT, the advantage of the hydrothermal synthesis of BST consists in a strong shift of the free energy toward much higher negative values compared to the classical ceramic route [47], according to values calculated with the HSC 7.1 thermodynamic software and presented in fig. 5.

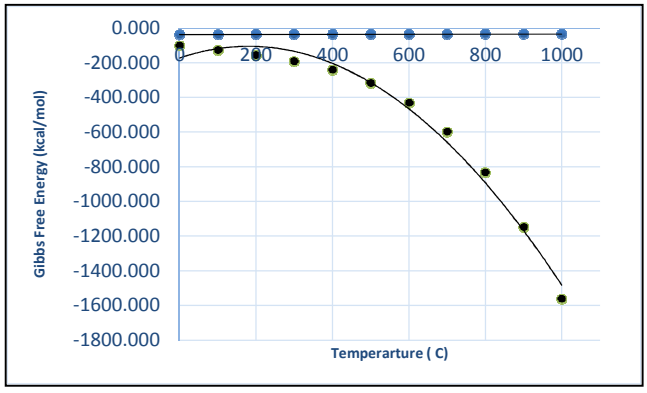

Fig. 5. The Gibbs free energy of formation of BST from oxides (upper straight line) and from aqueous ions (lower polynomial line) in hydrothermal solutions.

The perovskite $Ba_xSr_{1-x}TiO_3$ (x=0.7) based nanostructured materials were synthetized in one step process by hydrothermal method starting from soluble salts of Ti ($TiCl_4$ - Sigma ALDRICH – p.a. 98%), Sr ($Sr(NO_3)_2$ –MERCK- p.a. >99%), and $Ba(OH)_2*8H_2O$ (MERCK - p.a. >98%) and a mineralizer agent. Hydrothermal synthesis was performed in 5L Berghoff autoclave, at low temperatures (<200 ^{0}C) and high pressure (200 bar) for two hours.

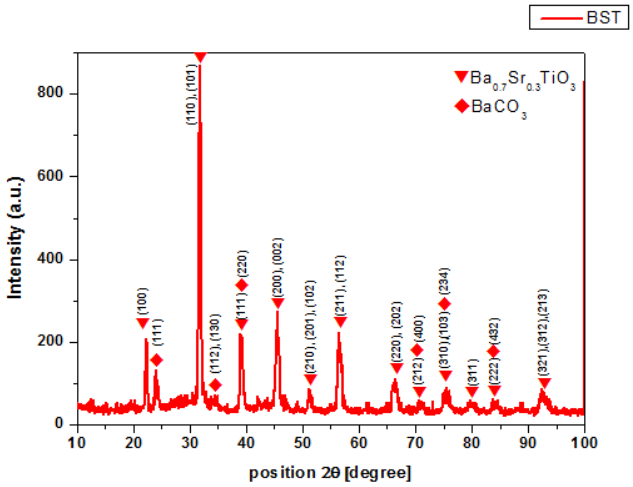

Fig. 6. XRD analysis on BST.

XRD analysis (Fig. 6) revealed the presence of two phases: $Ba_{0.7}Sr_{0.3}TiO_3$ (88.9%) indexed as tetragonal according to JCPDS No 04-015-0356 and $BaCO_3$ (11.1%) as orthorhombic according to JCPDS No. 00-005-0378. The average crystallite size is 19 nm. The tetragonality ratio (c/a) was 0.991. SEM analysis from Fig. 7 presents the BST powder having nanometer size ranging from 25 to 158 nm, with small particle tending to agglomerate.

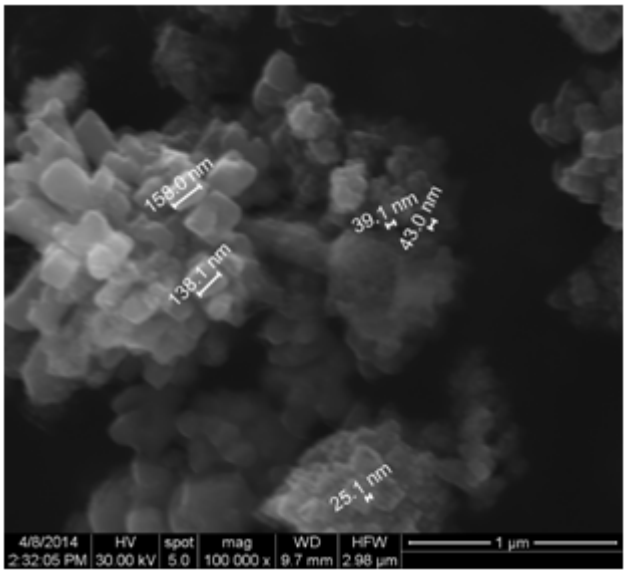

Fig. 7. SEM images for BST hydrothermally synthetized.

5. Hydrothermal/Solvothermal Synthesis of Nanostructured ZnO for Energy Storage Applications

The utilization of nanomaterials in thermal energy storage technologies is becoming more and more important as a radical solution for improving the performances of thermal systems and overcoming the problems of heat transfer [48]. Enhanced thermal transfer properties may be obtained by the utilization of very large specific surface area brought by the use of nanosystems. An innovative nanotechnological solution involves nanofluids obtained by micro/nano-encapsulation of phase change materials (PCMs) used to accumulate heat. It is well established that hexagonal ZnO (wurtzite) single crystals grow along the c axis and therefore (0001) surfaces are highly polar due to Zn^{2+}- and O^{2-}-terminated surfaces, while (001) surfaces are nonpolar [49]. Therefore, it is possible to explore the growth of nonpolar side surfaces of the (101) crystalline faces in view of obtaining inorganic shells or nanomatrices with simultaneous control of the hydrophobicity of the developed nanosystems. Nanoencapsulation in inorganic shells have been proposed recently as a method to encapsulate PCMs based on non-toxic sugar alcohol having a very high latent heat capacity [www.sam.ssa.eu]. D-Mannitol and Erythritol used as PCMs were encapsulated by a solvothermal process at high pressures and temperatures below 100^0C to avoid the melting of PCM. D-mannitol or erythritol, respectively were spray dried before hydrothermal synthesis in order to obtain as much as possible spherical shapes of sugar alcohol. The role of the high pressures is to enhance the encapsulation degree and stability of the nanomatrix by creating polar interactions between the –OH groups of sugar alcohols and Zn^{2+} ions from the shell.

Zinc nitrate hexahydrate was precipitated in aqueous medium with ammonia solution at alkaline pH. Precipitated white slurry representing ZnO precursor was further mixed in ethanol medium with spray dried D-mannitol or erythritol, respectively and hydrothermally treated at 100^0C for 1-3 hours at pressure of 40-3000 atm. Molar ratio between ZnO and mannitol was varied. Molar ratio between ZnO and erythriol was 4:1.

The FT-IR spectra of the erythritol encapsulated in ZnO from Fig. 8 identified stretching vibrations of O-H group (3260 cm^{-1}), C-O group (1079 cm^{-1}) and bending vibration of C-H group (2907 cm^{-1} and 1383 cm^{-1}) due to the presence of the sugar alcohol. The SEM picture from Fig. 9 shows the nucleation and growth of ZnO nanoparticles shell around the encapsulated erythritol.

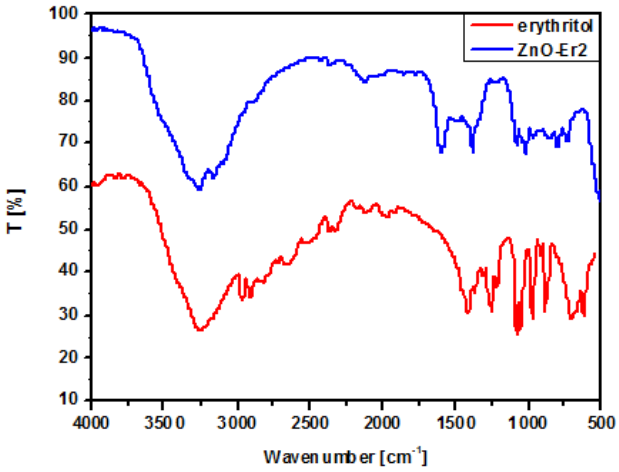

Fig. 8. FT-IR spectra of ZnO-Erythritol.

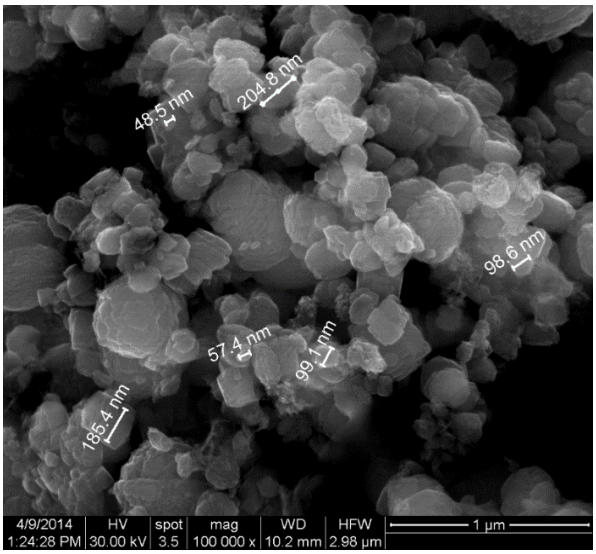

Fig. 9. SEM image of ZnO shell.

Analysis of the thermal behavior of the PCM based on Erythritol encapsulated in ZnO shell presented in Fig. 10 shows that during repeated heating and cooling cycles during direct scanning calorimetry measurements (DSC) the difference between the melting and solidification temperatures is maintained and the heat storage capacity is thus preserved.

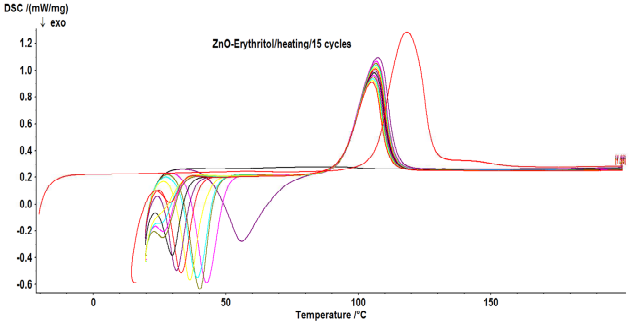

Fig. 10. DSC analysis showing thermal stability of Eyrthritol encapsulated in ZnO.

Modelling the encapsulation process of D-Mannitol in ZnO shell by high pressure solvothermal process at pressures between 100 and 3000 atm and 100^0C revealed that 1000 atm is the optimal pressure for obtaining a good encapsulation degree without degradation of the morphology and thermal properties of the encapsulated PCM. This innovative route for obtaining hybrid nanocapsules may open new directions in the seasonal thermal energy storage systems.

6. Conclusions and Future Prospects

Hydrothermal method is one of the chemical synthesis routes with high potential for obtaining nanostructured materials with controlled properties for energy harvesting applications. A large number of pure or doped oxide and non-oxide ceramic nanomaterials from mono-component and poly-component systems with properties required in sensors, actuators or devices were already reported. The main advantage of the hydrothermal processes is the ability to control nucleation and growth in complex systems containing a large number of components and dopants, without affecting the structural and morphological homogeneity. This is leading to important technological and environmental advantages compared to classical ceramic routes: one step process for direct production of crystalline nanomaterials, low energy consumption, products with much higher homogeneity, versatility in producing oxides, non-oxides, organic/biologic materials, hybrid materials with different morphologies, possibility to be up-scaled to pilot and production levels. To fully exploit these advantages in developing nanomaterials with controlled chemical, structural and morphological composition the experimental approach needs to start from thermodynamic prediction of equilibria in aqueous solutions, to study the kinetic of the process for controlling grain growth and model the synthesis leading to optimization of the whole process. These features are proved for some selected nanomaterials with high impact in energy harvesting technologies.

YTZP powders with crystallite sizes in the range 8–22 nm have been obtained by hydrothermal treatment of amorphous hydrous oxides. The crystallization degree increases with hydrothermal treatment temperature, agglomeration degree decreasing with temperature increasing and pH decreasing. The effective ionic conductivity of YTZP bulk materials was measured using impedance measurements**.** The contributions of bulk and grain boundaries on the total ionic conductivity were calculated and modelled from the impedance spectra of samples. The results on the activation energy of ionic conduction show a good agreement with the estimated values for YTZP nanomaterials.

Lead zirconate titanate (PZT) powders for piezoelectric materials in sensors, transducers and actuators were obtained. Prediction of free Gibbs energy of formation show a strong shift toward much higher negative values, compared to classical ceramic route. The thermodynamic design of PZT materials show the ability of hydrothermal process to produce PZT powders with crystalline sizes < 43 nm by modeling crystallite growth.

Similar to PZT case, hydrothermal synthesis of barium strontium titanate (BST) nanopowders allows a strong shift of the free energy toward much higher negative values compared to the classical ceramic route. Perovskite $Ba_xSr_{1-x}TiO_3$ (x=0.7) nanostructured powders with nanometer size ranging from 25-158 nm and tetragonality ratio (c/a) 0.991 were synthetized in one step process by hydrothermal method for future development of new types of sensors. Finally an innovative process for high pressure solvothermal encapsulation of some phase change materials based on sugar alcohols in zinc oxide nanomatrices for energy storage application was presented. Modelling the encapsulation process of D Mannitol in ZnO shell by high pressure solvothermal process at pressures between 100 and 3000 atm at 100^0C revealed that 1000 atm is the optimal pressure for obtaining a good encapsulation degree with no degradation of the morphology and thermal properties of the encapsulated PCM.

The development of such complex materials was based on thermodynamic approaches to predict the temperature and composition ranges and modelling methods to optimize the grain size and microstructure. Based on these approaches,

future developments are expected to show the scalability of the processes from laboratory to pilot and industrial scale, thus opening new directions in the energy harvesting field.

Acknowledgments

We gratefully mention:

- Financial support from European Commission in the frame of FP7- Fo.NMP.2013-11,
- Grant agreement no. 608720 "MicroFAST" for works on hydrothermal synthesis of PZT nanomaterials
- Financial support from Executive Unit for Financing Higher Education, Research,
- Development and Innovation (UEFISCDI) for support of works on hydrothermal synthesis of BST nanomaterials in the frame of grant no. 198/2012 SENSGAZ.
- Financial support from European Commission in the frame of FP7-Energy.2011-grant
- Agreement no. 296006 "SAM.SSA" for works on solvothermal encapsulation of phase change sugar alcohols in zinc oxide nanomatrices.

References

[1] Integrated Research and Industrial Roadmap for European Nanotechnology, 2012

[2] Carl C. Koch, Nanostructured Materials: Processing, Properties and potential Applications, 2002, Noyes Publications, USA, ISBN: 0-8155-1451-4

[3] P. Kriygsman, The Hydrothermal Synthesis of Ceramic Powders, Copyright by Chemical Engineering Company AG, Niederscherli, 1992, Switzerland

[4] D. Segal, Chemical Synthesis of Advanced Ceramic Materials, 1989, Cambridge University Press

[5] K.S. Pitzer, Activity Coefficients in Electrolyte Solutions, 2nd edn, CRC Press, (1991)

[6] Marioara Abrudeanu, Robert Piticescu, Roxana Piticescu, Sinteza chimica a pulberilor ceramice ultradisperse, Ed. Tehnica, 2000, Bucuresti

[7] H. Hayashi, Y. Hakuta, Materials 3(2010), 3794-3817; doi:10.3390/ma3073794

[8] H. Hayashi, K. Torii, J. Mater. Chem. 12(2002), 3671–3676.

[9] B. Li, Y. Hakuta, H. Hayashi,. J. Supercrit. Fluid. 39 (2006), 63–69.

[10] B. Li, Y. Hakuta, H. Hayashi, Mater. Lett. 61 (2007) 3791–3794

[11] M. Sorescu, L. Diamandescu., D. Tarabasanu, J. Phys. Chem. Solids 65 (2004), 1719–1725

[12] J. Lee, A.S. Teja, J. Supercrit. Fluid. 35(2005), 83–90

[13] M. Umetsu, X. Man, K. Okuda, M. Tahereh, S. Ohara, J. Zhang, S. Takami, T. Adschiri, Chem. Lett. 2006, 35, 732–733

[14] Q.X. Zheng, B. Li, M. Xue, H.D. Zhang, Y.J. Zhan, W.S. Pang, X.T. Tao, M.H. Jiang, J. Supercrit. Fluid. 39(2006), 63–69.

[15] D. Zhao, E. Han, X. Wu, H. Guan, Mater. Lett., 60(2006), 3544–3547.

[16] C.B. Xu, A.S. Teja, J. Supercrit. Fluid. 39(2006), 135–141.

[17] M.J. Yoon, J.H. In, H.C. Lee, Korean J. Chem. Eng. 23(2006), 842–846.

[18] D. Zhao, X. Wu, H. Guan, E. Han, J. Supercrit. Fluid 42(2007), 226–233.

[19] H. Assaaoudi, Z. Fang, I.S. Butler, D.H. Ryan, J.A. Kozinski, Solid State Sci. 9 (2007), 385–393.

[20] H. Assaaoudi, Z. Fang, I.S. Butler, J.A. Kozinski, Nanotechnology 19(2008), 185606.

[21] Akira Yoko, Makoto Akizuki, Yoshito Oshima, Journal of Nanoparticle Research, Volume 16, Issue 4(2014).

[22] Qian, Qian; Liu, Yin; Chen, Chen; Zhang, Peiliang; Jiao, Baoxiang; Hou, Guihua, Asian Journal of Chemistry, Volume 26, Issue 6(2014)

[23] W.L. Suchanek, R.E. Rieman, Advances in Science and Technology, 45(2006), p.184-193

[24] W-. Yao, S-H. Yu, Int. J. Nanotechnology, Vo. 4, No.1/2, (2007), p. 129-141

[25] T.R. Shrout, S.J. Zhang, J. Electroceramics 19(2007), 111-124

[26] S.P. Beeby, R.N. Torah, M.J. Tudor, P. Glynne-Jones, T.O' Donnell, C.R. Saha, S. Roy, J. Micromechanics and Microengineering 17(2007), 1257-1265

[27] D.J. Inman, Energy Harvesting Materials, 2009, Springer, ISBN 978-0-387-76463-4

[28] T. Dietl, Nature Mater., 9(2010), 965

[29] F.T. Ciachi and S.P. Badwal, J. Eur. Ceram. Soc., 7(1991), 197–206

[30] I. Kosacki, P. Colomban and H.V. Anderson, Proceedings of the US–Japan Workshop on Electrically Active Ceramic Interfaces. MIT, USA, 1998, pp. 180–188

[31] M. Miyayama and H. Yanagida, J. Am. Ceram. Soc., 67(1984), C194–C195

[32] Kim, B; Cho, K; Choi, J; Shin, D, J. Nanoscience and Nanotechnology, 15, Iss 1(2015)

[33] Zohreh Shahnavaz, Pooria Mn, Yatimah Alias, Ninie S.A. Manan. Sensors and Actuators B 208(2015) 389–398

[34] Hazhir Teymourian, Abdollah Salimi, Somayeh Firoozi, Aazam Korani, Saied Soltanian. Electrochimica Acta 143(2014) 196–206

[35] Luping Xue[a,1], Chenfei Shen[a, 1], Mingbo Zheng[b], Hongling Lu[a], Nianwu Li[a], Guangbin Ji[a], Lijia Pan[b] and Jieming Cao, Materials Letters, 65, Issue 2(2011), 198-200

[36] Pampuch, K. Haberko, Ceramic Powders, 1983, 623 – 634

[37] R. Stevens, Zirconia and zirconia ceramics, Magnesium Electron Ltd., ed. II, 1987

[38] Zhitomirsky, I., J. Eur. Ceram. Soc.,19(1999), 2581–2587

[39] R.R. Piticescu, C. Monty, D. Taloi, A. Motoc, S. Axinte, J. Eur. Ceram. Soc., 21(2001), 2057-2060.

[40] R.M. Piticescu, R.R. Piticescu, D. Taloi, V. Badilita, Nanotechnology, 14(2003), 1-6

[41] R.R. Piticescu, C. Monty, D. Millers, Sensors and Actuators B 109(2005), 102-106

[42] N. Settler, Ed., Piezoelectric Materials in Devices, ISBN 2-9703436-0-3, EPFL, 2002

[43] Mandel, C., Maune, H.; Maasch, M.; Sazegar, M.; Schüssler, M.; Jakoby, R. , Microwave Conference (GeMIC), 2011 German, ISBN: 978-1-4244-9225-1

[44] Dinghua Bao, Zhihong Wang, Wei Ren, Liangying Zhang, Xi Yao, Ceramics International 25(1999) 261-265

[45] R. M. Piticescu, P. Vilarhinho, L.M. Popescu, R.R. Piticescu, Journal of Optoelectronics and Advanced Materials, vol 8, no. 2(2006), 543-547

[46] S. Fuentes, F. Cespedes, L. Padiilla-Campos. D.E. Diaz-Droguett, Ceramics International 40(2014) 4975-4984

[47] Juan Li, Dengren Jin, Lixin Zhou, Jinrong Cheng, Materials Letters, Vol. 76, 2012, 100–102

[48] H. H. Al-Kayiem, S.C. Lin, A. Lukmon, Nanoscience & Nanotechnology-Asia, 3, 1(2013), 1-11

[49] Q. Ahsanulak, S.H. Kim, J.H. Kim, Y.B. Hahn, Mater. Res. Bull, 43 (2008), 3483-3489